Supporting Information

Exploring anisotropic properties of chiral nematic cellulose nanocrystal aerogels: Outstanding directional mechanical strength and unexpected surface-dependent thermal conductivity

Zongzhe Li[a], Karl Tsang[a], Yi-Tao Xu[a], James G. Drummond[b,c], D. Mark Martinez[b,c] and Mark J. MacLachlan[a,d,e,f]*

[a]Department of Chemistry, University of British Columbia, 2036 Main Mall, Vancouver, British Columbia, Canada V6T 1Z1

[b]Department of Chemical and Biological Engineering, University of British Columbia, 2360 East Mall, Vancouver, British Columbia, Canada V6T 1Z3

[c]Pulp and Paper Centre, University of British Columbia, 2385 East Mall, Vancouver, British Columbia, Canada V6T 1Z4

[d]Stewart Blusson Quantum Matter Institute, University of British Columbia, 2355 East Mall, Vancouver, British Columbia, Canada V6T 1Z4

[e]WPI Nano Life Science Institute, Kanazawa University, Kanazawa 920-1192, Japan

[f]Bioproducts Institute, University of British Columbia, 2385 East Mall, Vancouver, British Columbia, Canada V6T 1Z3

* mmaclach@chem.ubc.ca

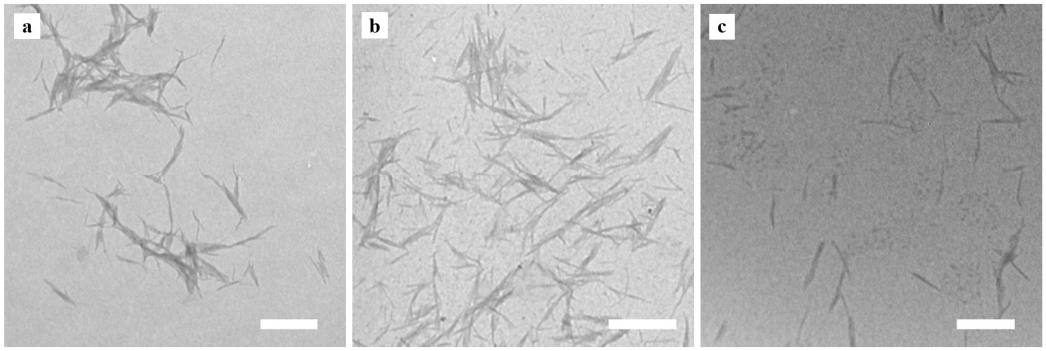

Figure S1. Transmission electron micrographs of CNCs from (a) the uniform CNC suspension, (b) the anisotropic phase of CNC suspension, and (c) the isotropic phase of CNC suspension. ImageJ (NIH, http://imagej.nih.gov/ij/) was used to manually measure CNC lengths and widths. Scale bar represents 500 nm for (a) and (b), 300 nm for (c).

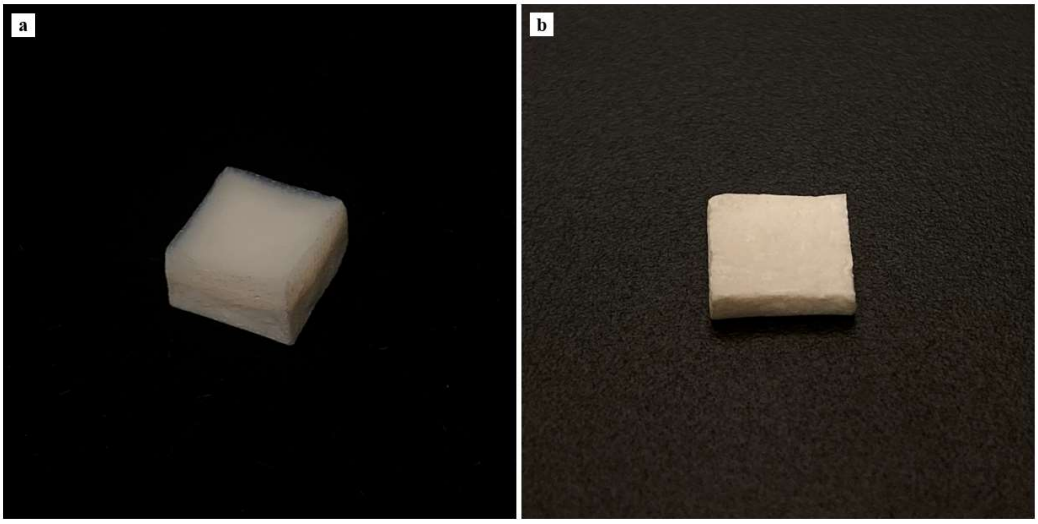

Figure S2. *cn*-CNC-C sample (a) before and (b) after slicing off the top part.

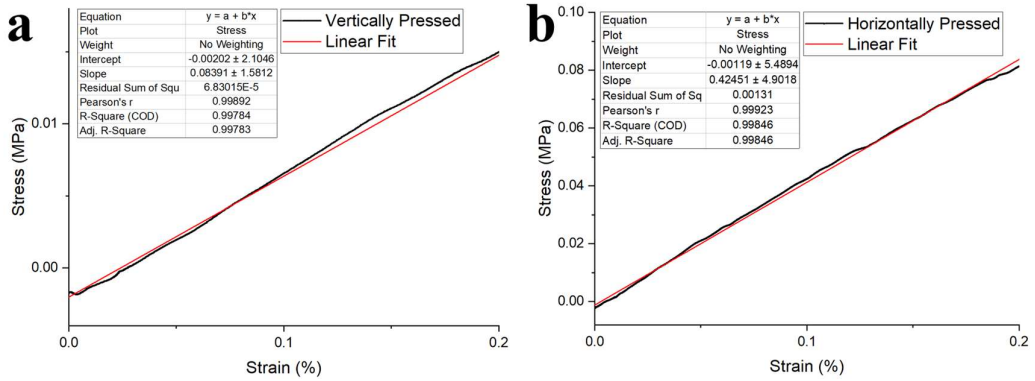

Figure S3. Linear regression analysis for representative stress-strain curves achieved from (a) vertical and (b) horizontal compression tests.

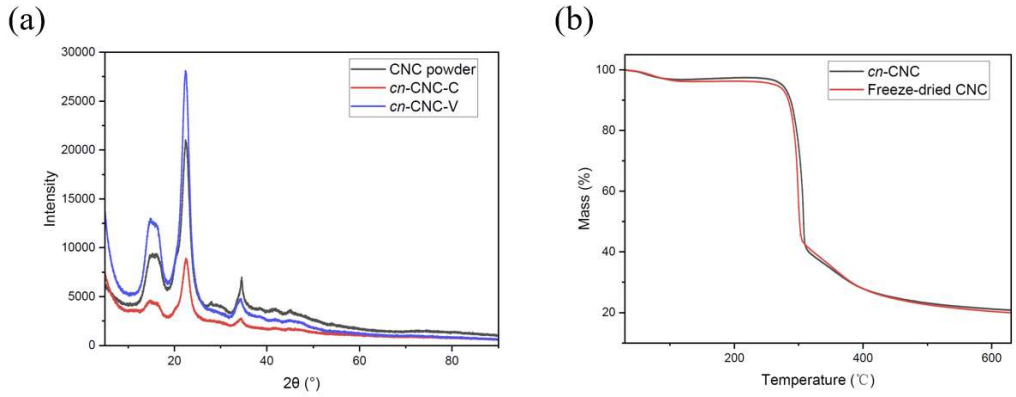

Figure S4. (a) Powder X-ray diffractograms of *cn*-CNC aerogels and freeze-dried CNC powder. Both display peaks characteristic of crystalline cellulose. (b) TGA curves of *cn*-CNC aerogel and freeze-dried CNC (nitrogen atmosphere; 10 °C/min). Both of them show similar thermal stability.

Table S1. Calculated density and porosity of *cn*-CNC-V

Diameter [mm]	Thickness [mm]	Weight [mg]	Density [g cm^{-3}]	Porosity [%]
21.5	1.83	92.4	0.139	91.5

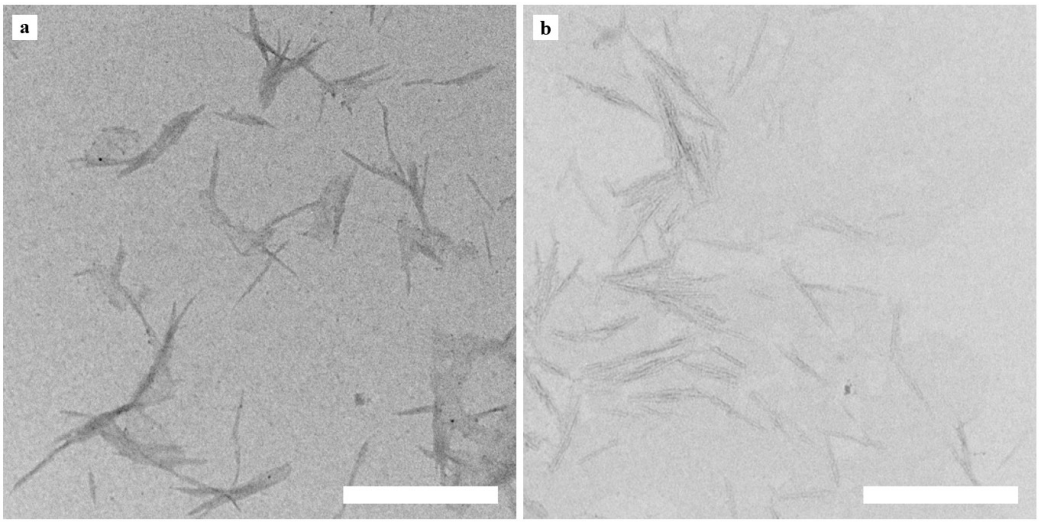

Figure S5. Transmission electron micrographs of CNCs from (a) the top part and (b) the bottom part of *cn*-CNC-V. ImageJ (NIH, http://imagej.nih.gov/ij/) was used to manually measure CNC lengths. Scale bar represents 500 nm.

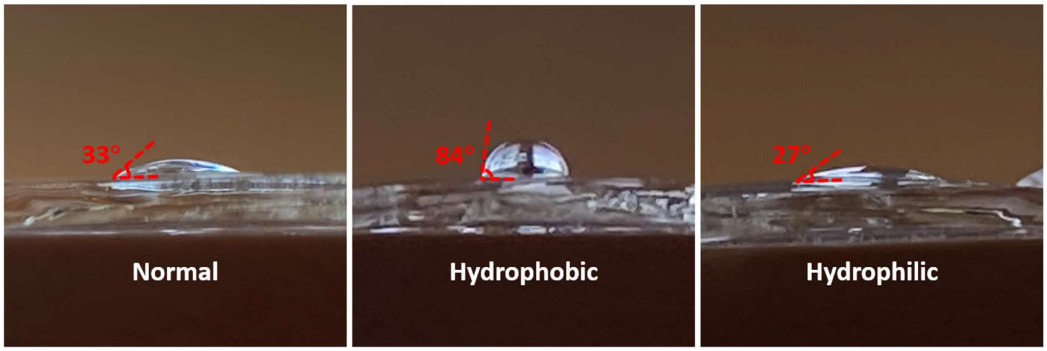

Figure S6. Photographs of (a) normal vial, (b) hydrophobic vial and (c) hydrophilic vial with a 5 µL droplet of water. Red dotted lines indicate water contact angles. ImageJ (NIH, http://imagej.nih.gov/ij/) was used for the analysis.

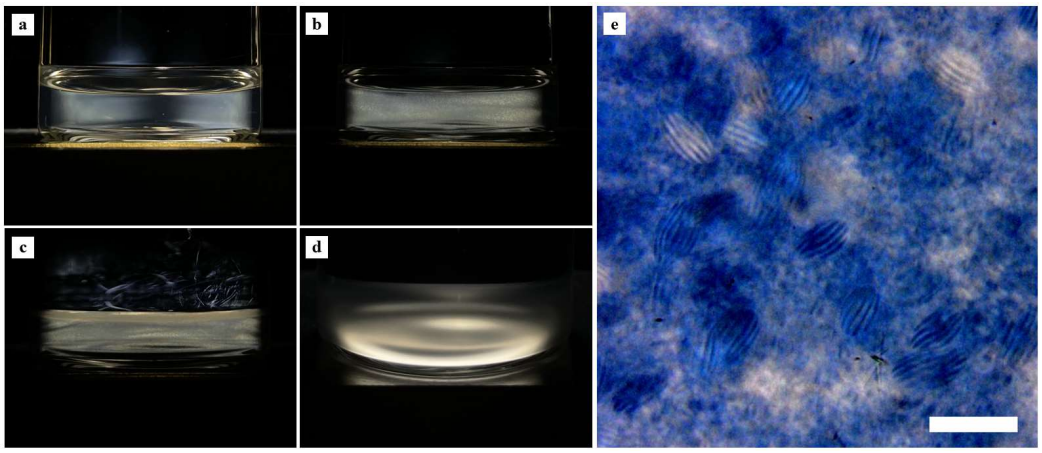

Figure S7. Time lapse study of isotropic CNC sample with equilibration. (a) After sonication, (b) after 24 h equilibration, (c) after adding ethanol, (d) after the gelation, and (e) POM micrograph of this equilibrated isotropic alcogel, showing tactoids as oval areas with fingerprint textures. Images shown in (a-c) are viewed between crossed polarizers. Scale bar represents 50 µm.

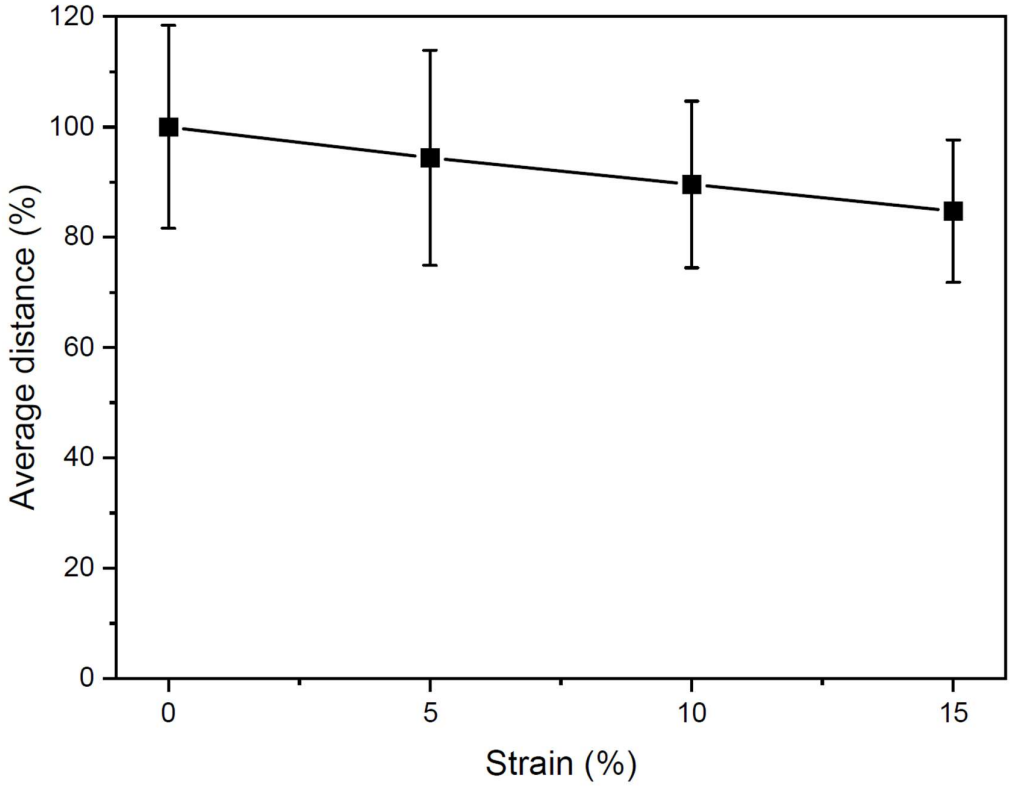

Figure S8. The relationship between average distance between CNC pseudolayers (corresponding to half helical pitch) with vertical strain applied to the material. ImageJ (NIH, http://imagej.nih.gov/ij/) was used to manually measure the half helical pitch for the chiral nematic structure of the CNCs.